ORIGINALE ARTICLE ISSN 2429-5396

MINERALOGICAL CONTROLS ON LEAD MOBILISATION IN A BASEMENT TERRAIN: INTEGRATED GEOCHEMICAL AND PETROGRAPHIC EVIDENCE FROM AN ABANDONED MINE SITE, NORTH-CENTRAL NIGERIA

| Hammed, Rasheed [1,2]* | Abdullahi, Suleiman [3] | and | Waheed Gbenga, Akande [4] |

1. Department of Geology, PMB 65, Gidan Kwano Campus, Federal University of Technology, Minna, Nigeria |
2. Department of Geology, University of Ibadan, Ibadan, Oyo State, Nigeria |
3. Department of Geology, PMB 65, Gidan Kwano Campus, Federal University of Technology, Minna, Nigeria |
4. Independent Researcher (formerly with Department of Geology, Federal University of Technology, Minna, Nigeria) |

| DOI: 10.5281/zenodo.19462180 | Received February 30, 2026 | | Accepted March 29, 2026 | | Published April 7, 2026 | | ID Article | Rasheed-Ref1-4-22ajiras300326|

ABSTRACT

Background: Abandoned artisanal and small-scale mining (ASM) sites are recognised as persistent sources of heavy metal contamination in the environment. In crystalline basement terrains, a fundamental challenge is the robust distinction between geogenic and anthropogenic contributions to metal enrichment, particularly for lead (Pb), which poses well-documented neurotoxicological risks even at low exposure levels. The Jiko abandoned mine site in North-Central Nigeria, underlain by Precambrian basement rocks of the Pan-African schist belt, provides an important case study in which naturally elevated lithogenic Pb concentrations may be compounded by artisanal mining activities. **Objectives**: This study aimed to: (i) characterise the mineralogical and whole-rock geochemical composition of basement lithologies at the Jiko site; (ii) evaluate the degree of chemical weathering using the Chemical Index of Alteration (CIA); and (iii) constrain the relative contributions of geogenic versus anthropogenic sources to Pb enrichment in overlying soils and surface waters. **Methods**: Six representative rock samples were collected across the principal lithological units of the study area. Major element geochemistry was determined by energy-dispersive X-ray fluorescence spectrometry (ED-XRF). Bulk mineralogy was characterised by powder X-ray diffraction (XRD) on a PANalytical Empyrean diffractometer. Optical petrography of polished thin sections was performed in plane-polarised light (PPL) and cross-polarised light (XPL). The CIA was calculated from molar oxide proportions, with CaO corrected for non-silicate fractions. Pearson correlation analysis was applied between bedrock major oxides and soil Pb concentrations. **Results**: XRF data reveal an intermediate to mafic basement composition with elevated Fe_2O_3 (mean = 9.58 wt.%), TiO_2 (2.17 wt.%), and CaO (6.03 wt.%). XRD identifies quartz, phlogopite, and albite as dominant primary phases, with secondary goethite and hematite in more altered samples. CIA values range from 48.35 to 62.20 (mean = 54.15), indicating incipient to moderate chemical weathering. A strong positive correlation between MgO and soil Pb (r = 0.817) provides robust evidence for a predominantly geogenic Pb source. Petrographic observation reveals frayed biotite margins, feldspar sericitisation, and Fe-oxide grain-boundary coatings, consistent with progressive Pb release and secondary redistribution. **Conclusions**: Pb enrichment at the Jiko site is primarily controlled by basement mineralogy, particularly mica- and feldspar-bearing lithologies of the Pan-African schist belt, with artisanal mining acting as a secondary kinetic accelerant of mobilisation. The data define a three-stage source-to-sink pathway: lithogenic storage within primary silicate lattices; weathering-induced Pb^{2+} release during feldspar hydrolysis and mica alteration; and partial retention via adsorption onto secondary Fe oxyhydroxides, with residual transfer to soils and surface waters. These findings highlight the critical importance of integrating mineralogical, geochemical, and petrographic evidence in contamination assessment at ASM sites, and recommend Pb isotopic analysis and SEM-EDS microanalysis for refined source apportionment and evidence-based remediation.

***Keywords**: Lead (Pb) mobilisation; Basement complex geology; Mineralogical controls; Environmental geochemistry; Artisanal and small-scale mining (ASM); Source apportionment.*

1. INTRODUCTION

Mineral resources constitute a significant component of the natural wealth of many nations and are extracted from bedrock, unconsolidated sediments, and alluvial deposits for downstream processing and value addition (Obaje, 2009; Dold, 2014). However, metalliferous mining activities invariably generate large volumes of waste materials, including tailings, spoil heaps, and open mine voids, and may promote the formation of acid mine drainage (AMD), thereby facilitating the mobilisation of heavy metals (HMs) or potentially toxic elements (PTEs) from the lithosphere into soils, surface and groundwater systems, and biota (Adriano, 2001; Johnson & Hallberg, 2005; Alloway, 2013). These contaminants may subsequently enter the human food chain through bioaccumulation and biomagnification, posing significant environmental and public health risks via inhalation, ingestion, and dermal exposure pathways (Järup, 2003; Lanphear et al., 2005; Laidlaw & Filippelli, 2008).
Environmental geochemistry provides a robust framework for evaluating the distribution and enrichment of elements across multiple environmental media, including soils, waters, rocks, and biota, relative to defined geochemical baselines (Hawkes & Webb, 1962; Förstner & Wittmann, 1983; Reimann & Garrett, 2005). Importantly, geochemical anomalies are defined as statistically significant deviations from local background concentrations rather than from global crustal averages, which may not reflect site-specific lithological controls (Salminen & Tarvainen, 1997; Reimann & Filzmoser, 2000). Such anomalies may arise from both geogenic processes, including the weathering and oxidation of primary mineral phases, and

anthropogenic inputs such as mining, industrial, and agricultural activities (Adriano, 2001; Tchounwou et al., 2012; Alloway, 2013).

A key challenge in environmental geochemistry is not only the delineation of geochemical anomalies but also the robust apportionment of their sources. Distinguishing between geogenic and anthropogenic contributions is critical for understanding contaminant pathways, designing remediation strategies, and mitigating public health risks (Komárek et al., 2008; Ettler, 2016). Failure to accurately constrain contamination sources can have severe consequences, as demonstrated by well-documented heavy metal poisoning events. Notably, the Zamfara State (Nigeria) lead poisoning outbreak in Nigeria, linked to artisanal mining of galena-rich ores, resulted in widespread child mortality due to ingestion and inhalation of contaminated dust (Dooyema et al., 2012; Plumlee et al., 2013; Nota et al., 2025). A similar incident in Niger State (Nigeria) further underscores the vulnerability of mining communities to Pb exposure (Gottesfeld et al., 2019).

A range of approaches has been employed for heavy metal source apportionment. Classical geochemical indices such as the Enrichment Factor (EF), Geoaccumulation Index (Igeo), and Contamination Factor (CF) provide first-order assessments of elemental enrichment relative to background levels (Müller, 1969; Håkanson, 1980; Sutherland, 2000). Multivariate statistical techniques, including correlation analysis and principal component analysis, are widely used to infer potential source groupings based on elemental associations (Facchinelli et al., 2001; Liu et al., 2003). More advanced methods, such as Pb isotopic analysis and receptor modelling, offer improved resolution of contaminant sources but are often constrained by analytical and logistical limitations (Komárek et al., 2008; Ettler, 2016). Consequently, reliance on limited datasets without supporting mineralogical or petrographic evidence may lead to ambiguous interpretations. Recent work by Rasheed et al. (2026, in press) reported significant enrichment of trace metals, particularly Pb, in soils and surface waters around the abandoned Jiko mine site in North-Central Nigeria. These elevated concentrations are consistent with the occurrence of Pb-bearing mineralisation within the Precambrian basement complex of the region (Rahaman, 1988; Obaje, 2009). While previous investigations such as Rasheed et al. (2026, in press) employed geochemical indices (e.g., EF, Igeo, CF) to assess contamination levels, the mineralogical controls on Pb mobilisation remain insufficiently constrained. This study therefore builds upon earlier work by integrating petrographic analysis, X-ray diffraction (XRD), and major element geochemistry to evaluate the role of basement lithology in controlling Pb mobilisation. The specific objectives are to: (i) characterise the mineralogical composition of rocks underlying the study area; (ii) assess the extent of chemical weathering using alteration indices; and (iii) constrain the relative contributions of geogenic and anthropogenic sources to Pb enrichment. By adopting a multi-proxy approach, this study aims to provide a more robust understanding of Pb mobilisation mechanisms and to support environmental risk assessment and management of abandoned mine sites in basement terrains.

2. MATERIALS AND METHODES

2.1 The Study Area and Geological Settings

The study area is centred on Jiko village in Munya Local Government Area, Niger State, North-Central Nigeria, within the Minna Sheet 164 of the Nigerian Geological Survey Agency (NGSA). It lies about 70 km northwest of Minna and close to the Niger–Kaduna State boundary, between latitudes 9°39′25.6″N and 9°42′26.2″N and longitudes 6°48′12.2″E and 6°49′23.0″E (Figure 1). Access is mainly through an untarred road and footpaths linked to the Minna–Mutum Daya road corridor.

The weather, topography, geomorphology and geology of the area have been comprehensively described in the recent geochemical studies by Rasheed et al. (2026, in press). Jiko lies within the Sudan–Guinea Savanna transition zone and experiences a tropical wet–dry climate with distinct rainy and dry seasons. The rainy season extends broadly from April to October, with peak rainfall in August–September, whereas the dry season spans November to March and is influenced by the Harmattan. The area forms part of the North-Central Hydrological Area, and the terrain is gently undulating with low-lying fluvial plains linked to the River Niger basin. These topographic and drainage conditions favour surface runoff, sediment redistribution, and the lateral transport of mine-derived materials during intense rainfall events. Land use is dominated by subsistence agriculture, artisanal fishing, and both active and abandoned artisanal and small-scale gold mining.

Geologically, the area is underlain by Precambrian Basement Complex rocks, comprising granitic, gneissic, and schistose lithologies (Figure 1**b**). These rocks form part of the Nigerian Basement Complex and are locally associated with structurally controlled quartz-vein mineralisation, including auriferous and polymetallic vein systems. Field observations confirm the presence of mineralised quartz veins, weathered bedrock exposures, and extensive alluvial workings within the study area. Mechanical and chemical weathering of these vein systems, coupled with fluvial reworking, has contributed to the accumulation of placer deposits in channels and floodplains. Because basement lithologies may contain naturally elevated concentrations of trace metals relative to average upper crustal values, it is necessary to distinguish lithogenic inputs from mining-related redistribution. In the Jiko area, artisanal mining activities, including excavation, crushing, panning, and sediment reworking, have likely enhanced the liberation and mobilisation of Pb and other potentially toxic elements from primary mineralised bedrock into surrounding soils and surface waters. The occurrence of numerous open mine pits along channels and terraces provides clear field evidence of both active and legacy alluvial gold mining.

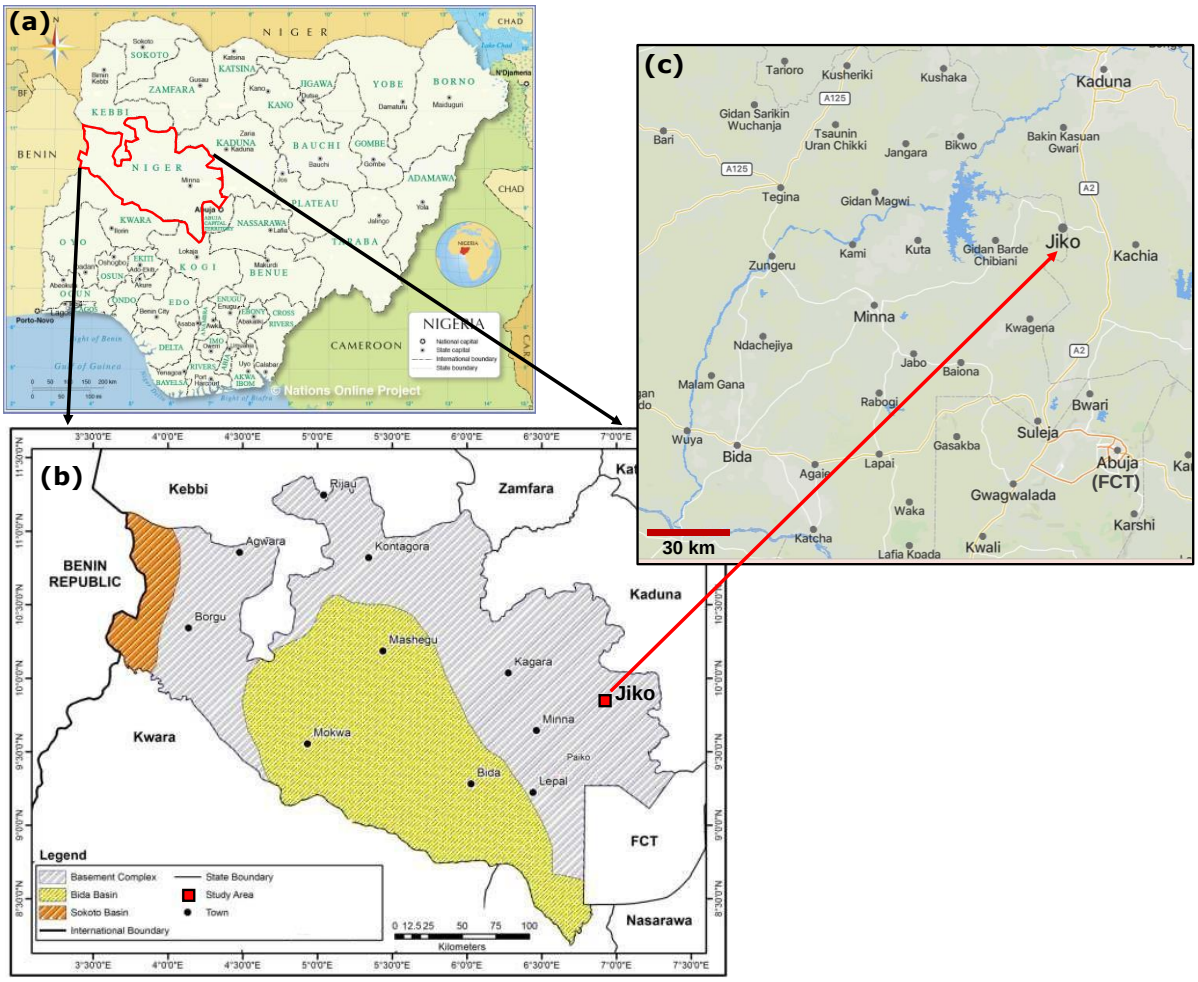

Figure 1: Location map of Jiko village in Munya LGA of Niger State, Nigeria [(**a**) Administrative Map of Nigeria (https://www.nationsonline.org/oneworld/map/nigeria-administrative-map.htm); (**b**) Geological Map of Niger State showing the Study Area (Modified after Ahmed et al., 2020); and (c) Jiko village on Mapcarta (https://mapcarta.com/33243376)].

2.2 Rock Sampling and Analytical Procedures

Field investigations were conducted at Jiko village between 15 April and 10 June 2019 to characterise the principal lithological units and associated mineralisation. Geological fieldwork involved reconnaissance mapping of exposed rocks, examination of quartz-vein systems, documentation of mine-related disturbances, and collection of representative rock samples for mineralogical and geochemical analyses. The geographic location details of the collected rock samples as measured by handheld GIS are as shown in Table 1. The analytical programme comprised X-ray fluorescence (XRF) for major element geochemistry, X-ray diffraction (XRD) for bulk mineralogical characterisation, and optical petrography of thin sections. Representative samples were collected from relatively fresh outcrops and mineralised vein materials across the study area. Sampling sites were selected to capture the main lithological units identified during mapping and, where possible, were located close to earlier soil sampling points to permit comparison between parent rock composition and overlying environmental media. Samples were collected using a geological hammer and chisel, and were described in the field based on colour, grain size, texture, fabric, visible alteration, and mineralisation. Geographic coordinates and elevations were recorded using a handheld GPS. A total of six rock samples (R1, R2, R2B, R3, R3B, and R4) were collected, labelled, bagged, and transported for laboratory analysis. Samples for XRF and XRD were analysed at the Nigeria Geological Survey Agency (NGSA), Kaduna, while thin sections were prepared at the NGSA Petrology Laboratory.

Table 1: Details of rock samples collected from Jiko and analysed in this work.

Sample Number	Latitude (Northings)	Longitude (Eastings)	Elevation (ASL, m)
R1	09039′55.33′′	006049′01.4′′	398
R2	09040′12.1′′′	006049′05.8′′	375
R2B	09039′54.7′′	006049′02.5′′	391
R3	09039′54.3′′	006049′04.0′′	398
R3B	09040′12.1′′	006049′05.8′′	375
R4	09039′56.0′′	006049′01.6′′	372

ASL: *Above sea level (in metres).*

2.2.1 Major Element Geochemistry by X-Ray Fluorescence (XRF)

Rock samples were first air-dried and then crushed and pulverised to fine powder. The powdered material was sieved to obtain a uniform grain-size fraction suitable for XRF analysis, after which the retained fraction was homogenised prior to subsampling. Approximately 5 g of each homogenised sample was loaded into a sample cup fitted with a thin support film for analysis. Major element analyses were carried out using a benchtop energy-dispersive X-ray fluorescence (ED-XRF) spectrometer at the NGSA Laboratory, Kaduna. The instrument was operated under analytical conditions appropriate for major oxide determination, with helium purge applied where necessary to improve sensitivity for lighter elements. Analytical results are reported as weight percent oxides, including SiO_2, TiO_2, Al_2O_3, Fe_2O_3, MnO, MgO, CaO, Na_2O, and K_2O normalised on a volatile-free basis.

2.2.2 Bulk Mineralogy by X-Ray Diffraction (XRD)

Bulk mineralogical composition was determined by powder X-ray diffraction (XRD) at the National Geosciences Research Laboratories (NGRL), Kaduna, using a PANalytical Empyrean diffractometer fitted with a Cu anode X-ray tube. The instrument was operated at 45 kV and 40 mA, with Cu Kα radiation ($K\alpha_1$ = 1.54060 Å, $K\alpha_2$ = 1.54443 Å). Data were acquired in continuous scan mode over a two-theta (2θ) range of 5.0024° to 74.9684°, using a step size of 0.0260° 2θ and a scan step time of 23.97 s. The diffractometer employed a flat sample stage in θ–θ goniometer geometry, with a goniometer radius of 240 mm and automatic divergence slit control.

Before analysis, samples were finely ground to reduce grain-size effects and improve representativeness of the bulk mineral assemblage. Powdered samples were packed into flat holders using a preparation procedure intended to minimise preferred orientation, especially in mica-rich samples. Diffracted intensity was recorded as a function of 2θ to produce characteristic diffractograms for each sample. Phase identification was carried out by matching observed peak positions and relative intensities with reference patterns in the ICDD Powder Diffraction File (PDF) database using HighScore Plus software. Mineral identifications were based on peak positions, d-spacings, and relative intensities, and were used to define the major rock-forming and accessory phases present in each sample.

2.2.3 Petrographic Analysis of Thin Sections

Representative samples were selected for thin-section preparation to examine mineral assemblages, grain relationships, textural features, and alteration patterns relevant to Pb mobilisation. Rock billets were cut from hand specimens, mounted on standard glass slides, and ground to the conventional petrographic thickness of about 30 µm at the NGSA Petrology Laboratory, Kaduna.

Thin sections were examined under an Olympus polarising petrographic microscope in the Department of Geology, Federal University of Technology, Minna, Nigeria using both plane-polarised light (PPL) and cross-polarised light (XPL). Petrographic observations focused on modal mineralogy, grain size and shape, grain-boundary relationships, foliation, vein textures, and evidence of alteration or replacement. Mineral identification was based on standard optical properties, including pleochroism, cleavage, birefringence, extinction behaviour, and interference colours (e.g., Nesse, 2013). Petrographic observations were cross-checked against XRD results to reconcile bulk mineralogy with textural and paragenetic relationships. Because reflected-light ore microscopy was not available, opaque ore minerals and their alteration products could not be examined in detail. Nevertheless, transmitted-light petrography provided important constraints on silicate mineral assemblages, weathering textures, and alteration features relevant to the interpretation of lithological controls on Pb mobilisation.

3. RESULTS

3.1 Major Element Geochemistry by X-Ray Fluorescence (XRF)

Major element compositions of the six analysed rock samples from the Jiko abandoned mine site are presented in Table 2. The samples are chemically dominated by SiO_2 and Al_2O_3, with subordinate Fe_2O_3, CaO, TiO_2, MgO, and minor alkali oxides. SiO_2 contents range from 50.64 to 64.15 wt.% (mean = 59.32 wt.%), indicating compositions broadly within the intermediate to moderately felsic range. Al_2O_3 concentrations are comparatively uniform, ranging from 15.21 to 16.21 wt.% (mean = 15.76 wt.%). Fe_2O_3 contents are relatively high, varying from 8.00 to 12.36 wt.% (mean = 9.58 wt.%), while TiO_2 ranges from 1.59 to 3.09 wt.% (mean = 2.17 wt.%). The highest TiO_2 values occur in R3 and R3B, consistent with the presence of Ti-bearing accessory phases subsequently identified by XRD. CaO ranges from 4.86 to 7.10 wt.% (mean = 6.03 wt.%), and MgO from 1.21 to 2.32 wt.% (mean = 1.72 wt.%). In contrast, K_2O and Na_2O occur at generally lower concentrations, with K_2O ranging from 0.12 to 1.41 wt.% (mean = 0.59 wt.%) and Na_2O from 0.37 to 1.89 wt.% (mean = 1.06 wt.%). MnO values are low overall (0.058-0.16 wt.%; mean = 0.10 wt.%), and loss on ignition (LOI) values are also low (0.90-1.32 wt.%; mean = 1.12 wt.%), indicating limited volatile content and generally low degrees of bulk alteration. Overall, the XRF dataset indicates that the analysed rocks are chemically heterogeneous but consistently enriched

in Fe and Ti relative to alkalis, with some samples showing stronger mafic to intermediate signatures than others.

3.1.1 Chemical Index of Alteration (CIA) and Weathering Status

The degree of chemical weathering of the basement rocks was assessed using the Chemical Index of Alteration (CIA), originally formulated by Nesbitt & Young (1982) and widely applied in environmental geochemistry and weathering studies of crystalline basement lithologies (McLennan, 1993; Taylor & McLennan, 1985):

$$CIA = \left[\frac{Al_2O_3}{Al_2O_3 + CaO^* + Na_2O + K_2O}\right] \times 100 \quad (1)$$

where all values are expressed as molar proportions and CaO* represents the CaO fraction associated exclusively with the silicate mineralogy, corrected for carbonate and apatite contributions following the procedure described by McLennan (1993). The CIA scale ranges from approximately 50 for completely fresh, unweathered primary feldspar-bearing rocks to 100 for residual materials composed entirely of Al-rich secondary clay minerals such as kaolinite (e.g., Nesbitt & Young, 1982). The calculated CIA values range from 48.35 to 62.20, with a mean of 54.15 (Table 3). These values indicate that the analysed rocks are fresh to slightly weathered overall, although some samples show higher degrees of alteration than others. The lowest CIA value occurs in R3 (48.35), indicating the least altered sample in the set, whereas the highest value occurs in R2 (62.20), indicating comparatively stronger chemical alteration. Intermediate values are recorded for R1 (51.27), R2B (55.21), and R3B (58.12), suggesting variability in weathering intensity across the sampled lithologies. The overall CIA range is consistent with the preservation of substantial primary silicate mineralogy alongside incipient to moderate chemical alteration.

Table 2: Major element geochemistry of rock samples from the Jiko abandoned mine site determined by ED-XRF spectrometry (values in wt.%).

Oxides (wt%)	R1	R2	R2B	R3	R3B	R4	Average
SiO_2	59.30	58.50	63.14	50.64	64.15	60.20	59.32
Al_2O_3	15.78	16.21	15.76	15.84	15.77	15.21	15.76
CaO	6.77	7.10	5.50	6.76	4.86	5.21	6.03
MgO	2.14	2.00	1.28	2.32	1.21	1.34	1.72
K_2O	0.48	0.45	0.90	1.41	0.12	0.16	0.59
Na_2O	1.32	1.29	1.10	1.89	0.37	0.40	1.06
TiO_2	1.59	1.61	1.64	3.09	2.66	2.40	2.17
MnO	0.10	0.12	0.079	0.16	0.058	0.061	0.10
Fe_2O_3	9.51	9.43	9.34	12.36	8.85	8.0	9.58
LOI	1.20	1.00	1.00	1.32	1.31	0.90	1.12

Table 3: Chemical Index of Alteration (CIA) values for analysed rock samples.

Sample	*CIA	Weathering Status
R1	51.27	Fresh to slightly weathered
R2	62.20	Slightly to moderately weathered
R2B	55.21	Slightly weathered
R3	48.35	Fresh
R3B	58.12	Slightly to moderately weathered
R4	49.75	Fresh to slightly weathered
Mean	**54.15**	**Incipient weathering**

*__CIA__ indicates the level of chemical weathering of sampled basement rocks (Rasheed et al., 2026, in press).

3.1.2 Correlation Between Rock Major Oxides and Soil Pb

Pearson correlation coefficients between selected major oxides in bedrock and Pb concentrations in soils are presented in Table 4. The strongest positive correlation is observed between MgO and soil Pb (r = 0.817), followed by CaO (r = 0.705). MnO (r = 0.541) and Fe_2O_3 (r = 0.390) show moderate positive correlations, whereas SiO_2 exhibits a moderate negative correlation (r = -0.526). K_2O and TiO_2 show negligible correlations with soil Pb. These relationships indicate that soil Pb concentrations vary systematically with some major oxide components of the bedrock, especially MgO and CaO, while others show little or no association.

Table 4: Pearson correlation coefficients between selected major oxides in basement rocks and Pb concentrations in soils.

Oxides	Correlation with Soil Pb (r)	Relationship
MgO	0.817	Very Strong Positive
CaO	0.705	Strong Positive
MnO	0.541	Moderate Positive
Fe_2O_3	0.390	Moderate Positive
SiO_2	-0.526	Moderate Negative
K_2O	0.053	Negligible
TiO_2	0.033	Negligible

3.2 Bulk Mineralogical Characterisation by X-Ray Diffraction (XRD)

Powder XRD analysis identified quartz, albite, and phlogopite as the principal mineral phases in the analysed rock samples (Figures 2-5; Table 5). Quartz occurs in all analysed samples and is represented by its characteristic strong reflections, including peaks near 20.86°, 26.64°, and 50.13° 2θ. It is the most consistently expressed phase across the diffractograms. Phlogopite is the second most prominent silicate phase and is identified by basal reflections near 8.9° 2θ and additional peaks in the 26-28° 2θ range. Albite is also present in most samples but is generally less abundant than quartz and phlogopite, in agreement with the relatively low Na_2O contents obtained from XRF. In addition to the primary silicate assemblage, several samples show evidence of secondary or alteration-related phases. Peaks attributable to goethite occur in some samples, especially around 21.2° 2θ, while reflections consistent with hematite are observed near 36.5° 2θ in the more altered samples. These Fe-oxide phases are most clearly expressed in R2B and R3B. Sample R3 also shows a distinct peak near 32.5° 2θ, consistent with the presence of ilmenite, in agreement with its elevated TiO_2 concentration. The diffractograms indicate mineralogical variation across the sample set, with some samples dominated by relatively fresh primary silicates and others showing additional secondary iron oxide phases. This pattern is consistent with variable degrees of alteration across the study area.

Table 5: Summary of XRD mineral assemblages and related observations for analysed rock samples.

Samples	Principal Phases	Secondary Phases	Notable Observations
R1	Quartz, phlogopite, albite	None detected	Sharp primary silicate peaks
R2	Quartz, phlogopite, albite	Fe-oxide/clay-related features	More altered pattern
R2B	Quartz, phlogopite, albite	Goethite	Early Fe-oxide development
R3	Quartz, albite, phlogopite	Ilmenite	Highest TiO_2; strong crystallinity
R3B	Quartz, phlogopite	Goethite, hematite	Strong secondary Fe-oxide peaks
R4	Quartz, phlogopite, albite	Minor alteration features	Intermediate character

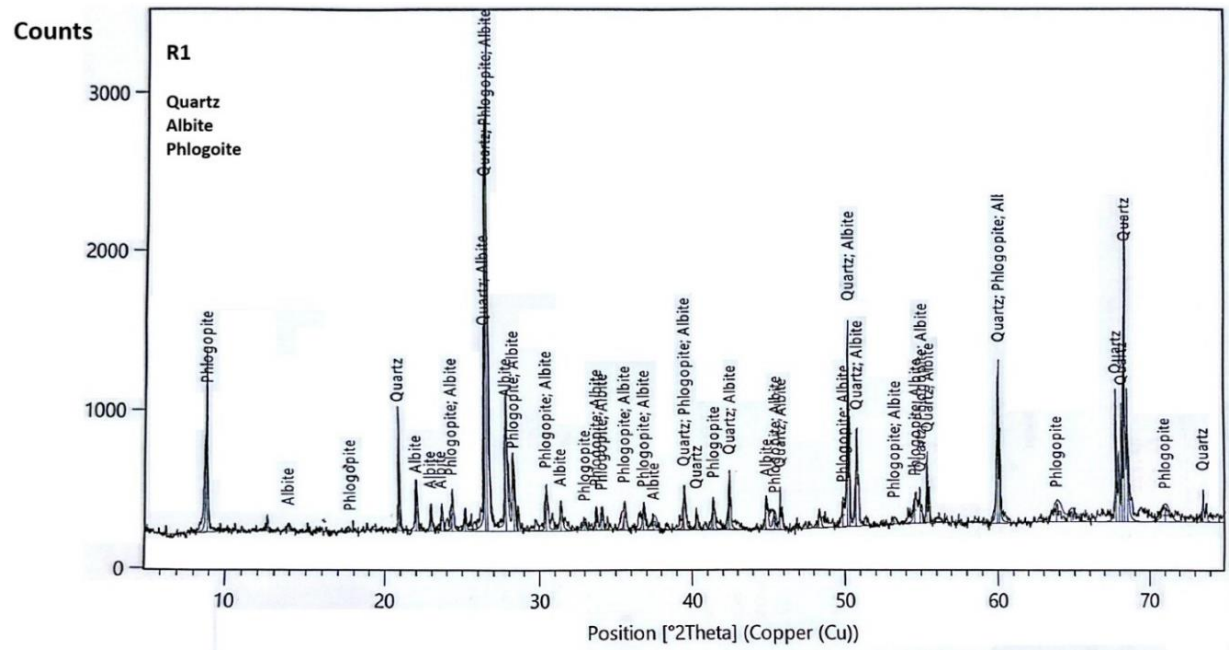

Figure 2: XRD diffractogram of sample R1 showing the main reflections of quartz, phlogopite, and albite.

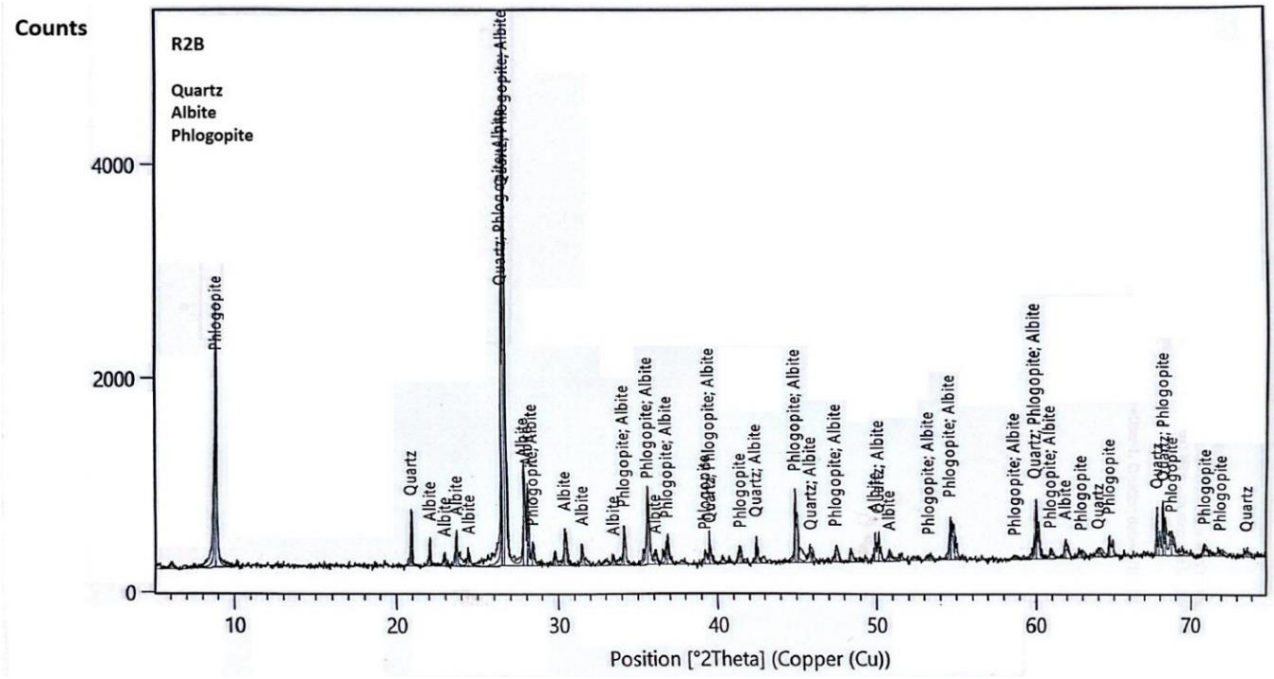

Figure 3: XRD diffractogram of sample R2B showing quartz, phlogopite, albite, and alteration-related peaks.

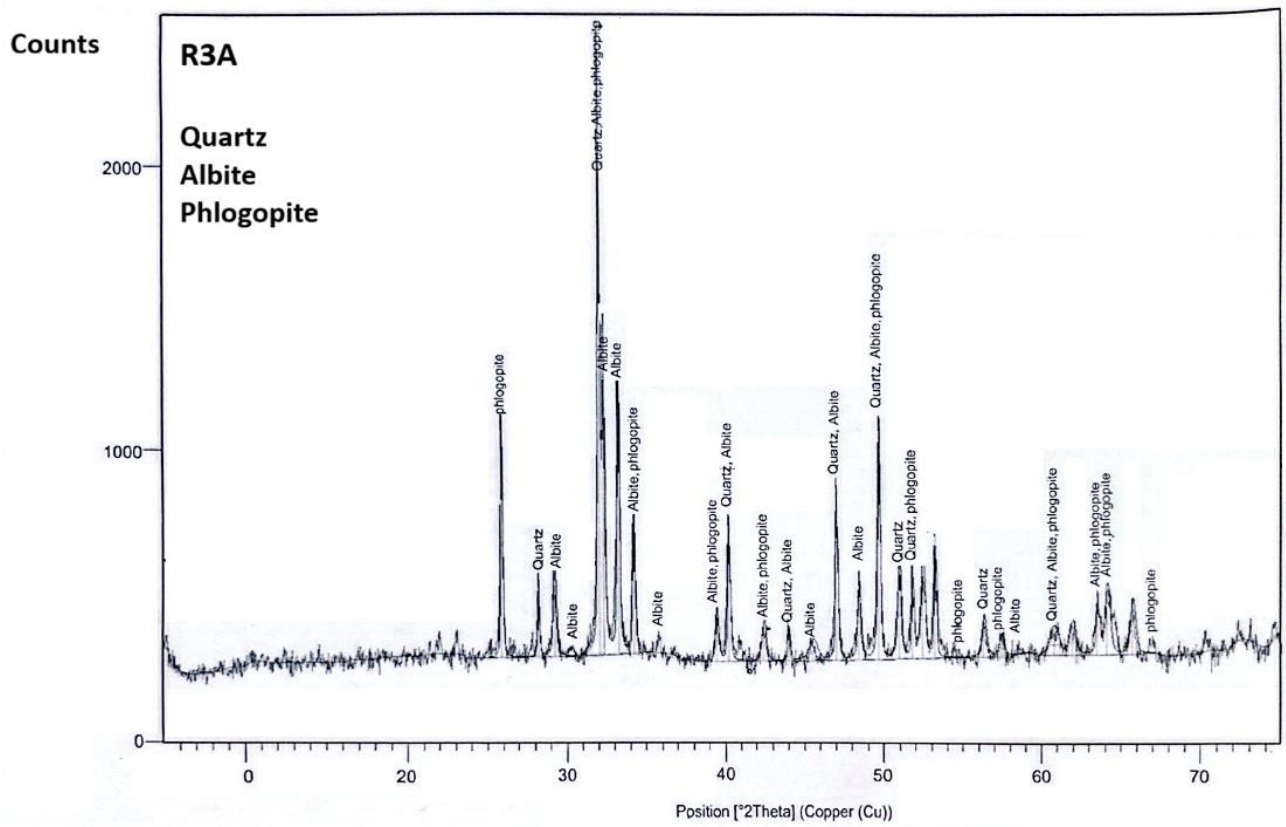

Figure 4: XRD diffractogram of sample R3 showing quartz, phlogopite, albite, and ilmenite-related reflections.

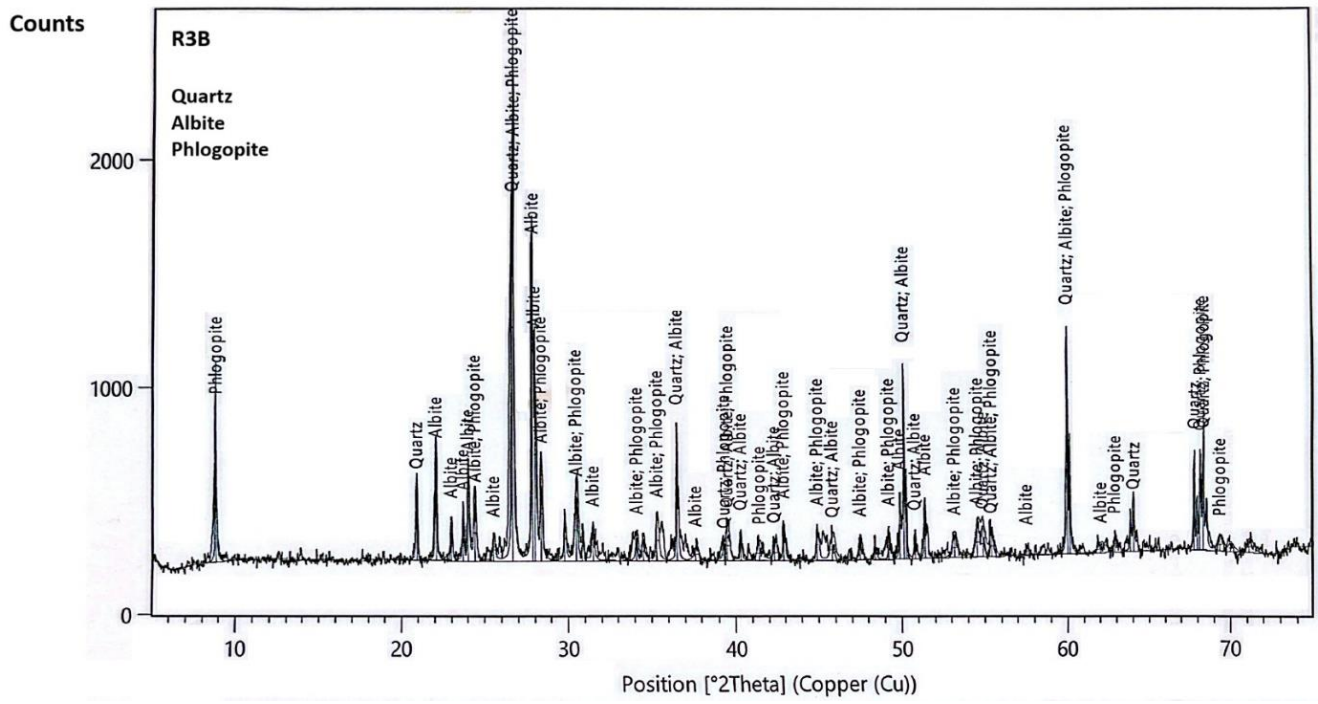

Figure 5: XRD diffractogram of sample R3B showing primary silicates and secondary iron oxide phases.

3.3 Petrographic Analysis

Petrographic examination of thin sections reveals two main lithological/textural domains in the analysed rocks: a schistose domain and a gneissic to more strongly altered domain (Figures 6-7; Table 6). These domains differ in mineral fabric, degree of mica alteration, feldspar turbidity, and abundance of iron oxide staining.

3.3.1 Schistose Domain

The schistose samples are characterised by a well-developed planar fabric defined by the preferred orientation of elongate mica grains, mainly biotite and muscovite, set within a quartz- and feldspar-rich matrix. Under plane-polarised light, biotite shows strong pleochroism from pale yellow to dark brown. Quartz occurs mainly as anhedral to subhedral grains, while feldspar is locally turbid and partly altered. A notable feature of this domain is the occurrence of frayed or ragged biotite margins, particularly along cleavage traces. Feldspar grains show incipient sericitisation, expressed as fine-grained alteration products and dusty internal turbidity. These features indicate that the schistose rocks preserve the primary mineral framework but also show clear evidence of early mineral alteration.

3.3.2 Gneissic to Altered Domain

The second domain is defined by a gneissic fabric with compositional banding between felsic and mafic components. Quartz and feldspar dominate the felsic bands, whereas biotite is concentrated in darker layers. Relative to the schistose domain, mica grains in this group are more strongly altered, more fractured, and commonly darker in transmitted light. Feldspar grains display more advanced turbidity and alteration, and grain boundaries are frequently coated or stained by iron oxide precipitates. In some sections, these oxide accumulations occur along fractures and intergranular boundaries, corresponding to the secondary Fe-oxide phases identified by XRD. The altered domain therefore records a stronger overprint of chemical weathering and secondary mineral formation than the schistose domain.

Table 6: Summary of key petrographic features observed in the analysed rocks.

Petrographic feature	Schistose domain	Gneissic/altered domain
Dominant fabric	Schistosity; aligned mica laths	Gneissic banding; felsic-mafic segregation
Main minerals	Quartz, biotite, muscovite, plagioclase	Quartz, feldspar, biotite
Biotite condition	Pleochroic; frayed margins	More fractured and altered
Feldspar condition	Incipient sericitisation; slight turbidity	Stronger turbidity and alteration
Grain boundaries	Generally clean to slightly stained	Common Fe-oxide coatings and staining
Alteration intensity	Low to moderate	Moderate to relatively advanced

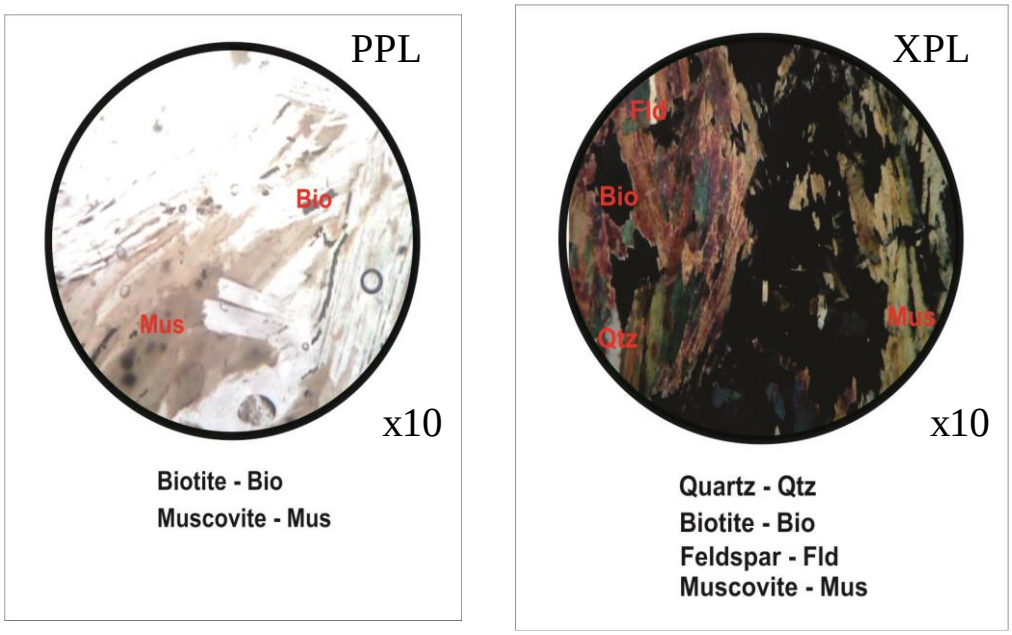

Figure 6: Photomicrographs of representative schistose rock sample under PPL and XPL (Location 4; ×10).

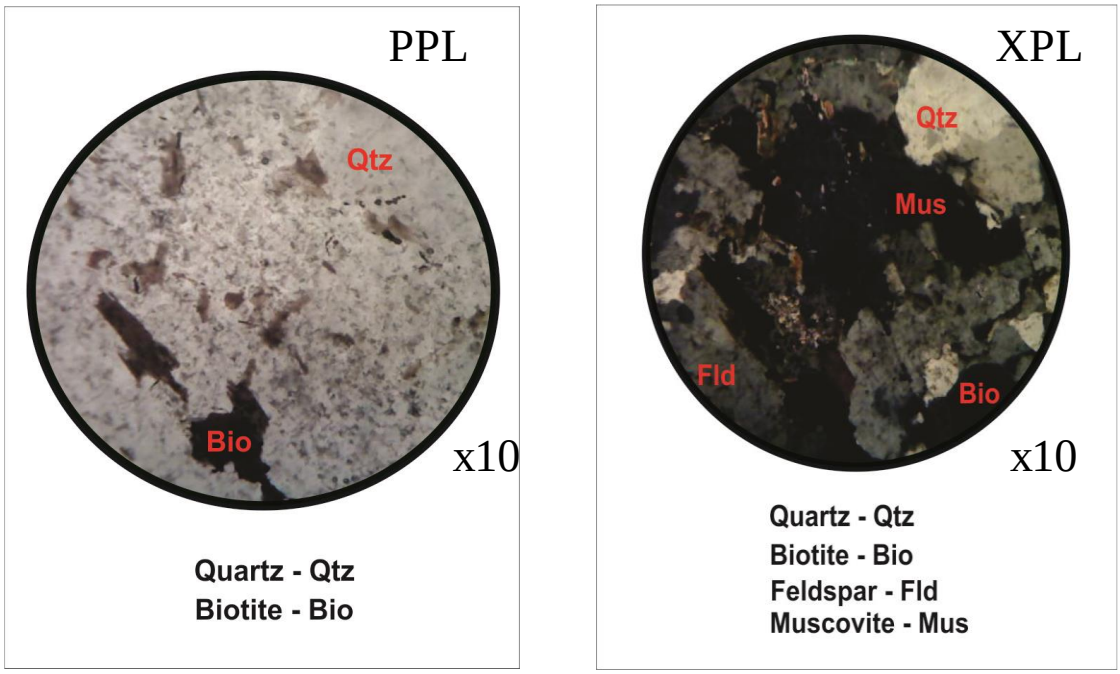

Figure 7: Photomicrographs of representative gneissic/altered rock sample under PPL and XPL (Location 5; ×10).

4. DISCUSSION

4.1 Whole-rock Chemistry and Lithological Affinity of the Jiko Basement

The major element geochemistry of the Jiko rocks (Table 2) indicates a mafic- to intermediate-influenced basement assemblage rather than a uniformly felsic granite-dominated composition. The moderate SiO_2 contents, elevated Fe_2O_3 and TiO_2, and relatively low alkali abundances collectively point to a lithological framework richer in ferromagnesian minerals and calcic feldspar than would be expected for average upper continental crust. This interpretation is consistent with the geology of the Nigerian Basement Complex, where schist belts and associated metaigneous and metasedimentary rocks commonly contain amphibolitic, schistose, and mica-rich lithologies with higher Fe-Ti-Mg contents than typical granitic crust (Rahaman, 1988; Garba, 2003; Obaje, 2009). It is also compatible with nearby lithological descriptions from Minna Sheet 164, where quartz-, mica-, oxide-, and aluminosilicate-bearing rocks have been reported in structurally complex basement units.

In environmental geochemical terms, this lithological context is important because naturally elevated trace-metal backgrounds are commonly associated with mafic minerals, Fe-Ti oxides, micas, and vein-related mineralisation. The elevated TiO_2 contents of samples R3 and R3B, coupled with XRD recognition of ilmenite, support the presence of a Fe-Ti-rich accessory mineral assemblage. Likewise, the relatively high CaO and MgO contents indicate that the bedrock contains significant proportions of Ca-Mg-bearing silicates and/or mica-rich phases, which are plausible hosts for trace Pb either by direct incorporation during crystallisation or by association with mineralised vein systems. Accordingly, the chemical data suggest that Pb enrichment at Jiko should not be treated a priori as an exclusively anthropogenic signal. Rather, the basement itself appears capable of supplying Pb to the surficial environment through weathering of mineralised and mafic-rich lithologies, with artisanal mining likely increasing the rate of release and dispersion. Comparable Pb enrichment linked to basement lithology and ASM disturbance has been reported in Nigeria (Garba, 2003; Gottesfeld et al., 2019) and across sub-Saharan African schist belts (Hilson, 2002; Ettler, 2016), although the magnitude of dissolved Pb at Jiko exceeds many reported cases, indicating enhanced mobilisation efficiency.

4.2 Weathering Intensity and the Significance of CIA Values

The CIA values (Table 3) indicate that the Jiko rocks are fresh to moderately weathered, and these values (50–65 CIA) indicate incipient but active silicate weathering capable of mobilising lattice-bound metals (Nesbitt & Young, 1982; McLennan, 1993), a process particularly effective in Tropical Savanna environments where seasonal hydrological flux enhances element leaching (Dold, 2014; Fashola et al., 2016). These values are important because they show that Pb mobilisation at Jiko does not require extreme or prolonged weathering of the bedrock mass. Instead, even modest hydrolytic alteration appears sufficient to initiate release of lattice-bound or structurally associated Pb from primary minerals. It is worth mentioning that we have made this interpretation with a caution. As emphasised by Algeo et al. (2025), CIA is most robust when interpreted together with mineralogical and petrographic evidence, because alkali loss, protolith composition, and secondary mineral formation can all influence bulk-rock weathering indices. In the present study, the CIA values are supported by thin-section evidence of feldspar turbidity, incipient sericitisation, and mica alteration, and by XRD detection of secondary Fe oxyhydroxides, which together confirm that the CIA signal reflects genuine mineralogical modification rather than a purely compositional artefact.

The relatively low K_2O and Na_2O contents of the rocks (Table 2) further support progressive depletion of mobile alkalis during alteration of feldspar and mica. In tropical and seasonally wet basement terrains, such early weathering commonly causes hydrolysis of feldspars and progressive destabilisation of mica cleavage domains, producing secondary clay minerals and Fe-rich alteration products. At Jiko, the CIA range therefore marks a weathering interval in which the rocks remain largely crystalline, but the first major geochemical transfer of Pb from primary mineral hosts to pore fluids and secondary sorbent phases is already underway.

4.3 Primary Mineralogical Controls on Pb Storage

The XRD and petrographic data together indicate that the dominant primary assemblage at Jiko is composed of quartz, albite, and phlogopite, with local oxide-rich phases such as ilmenite. Of these minerals, quartz is geochemically inert with respect to Pb storage and mainly acts as a diluting framework phase. In contrast, the mica- and feldspar-bearing components provide the most plausible lithogenic reservoirs for Pb. Phlogopite is particularly important in this respect. Trioctahedral micas can accommodate trace metals through lattice substitution and can also retain them along cleavage surfaces, inclusion boundaries, and interlayer defects. The strong positive correlation between MgO and soil Pb ($r = 0.817$; Table 4) therefore provides a compelling geochemical link between Pb distribution in the soil and the abundance of Mg-bearing basement minerals, especially mica-rich phases. Similar geogenic associations between Pb and mafic indicators have been reported in basement terrains (Reimann & Filzmoser, 2000; Facchinelli et al., 2001; Ettler, 2016). This interpretation is reinforced by petrographic evidence of biotite/phlogopite degradation and by the persistence of mica peaks in the less altered XRD patterns (Figures 6-7; Table 6).

Plagioclase, represented here chiefly by albite in the XRD data, is also relevant, although probably as a secondary rather than dominant Pb host. Feldspars may incorporate trace Pb during crystallisation and subsequently release it during hydrolysis, especially where fractures, sericitic replacement, and fluid access accelerate dissolution. The presence of turbid and sericitised feldspar in thin-section supports this pathway (Figures 6-7). Thus, the data suggest that Pb at Jiko is stored mainly within the primary basement mineral assemblage, especially in mica-rich and feldspar-bearing lithologies, rather than existing solely as a detached contamination product from surface mining operations.

4.4 Secondary Fe Oxyhydroxides as Sinks and Carriers of Pb

The appearance of goethite and hematite (Figures 4-5) in the altered samples is one of the most important mineralogical results of this study. These minerals indicate progressive oxidation of Fe-bearing primary phases and, at the same time, provide a strong geochemical explanation for the partitioning of Pb between rocks, soils, and waters. Goethite and hematite are highly effective scavengers of trace metals because their hydroxylated surfaces provide abundant sites for adsorption and surface complexation. Goethite exhibits strong affinity for Pb^{2+} via inner-sphere complexation (Tessier et al., 1979;

Cornell & Schwertmann, 2003), a mechanism widely documented in mine-impacted soils and sediments (Ettler, 2016; Fashola et al., 2016). In mining-affected and weathered basement terrains, Pb released from degrading micas, feldspars, and vein-related sulphides is commonly redistributed onto Fe oxyhydroxides, where it may be temporarily retained in the regolith or transported as fine-grained colloidal material. This behaviour is widely recognised in environmental geochemistry and mine-water systems, where Fe oxyhydroxides act both as sinks for dissolved metals and as secondary phases capable of releasing them again when pH or redox conditions change. In other words, under fluctuating redox conditions, Fe–Mn oxides may alternately act as sinks and secondary sources of Pb, releasing adsorbed metals during reductive dissolution (Hudson-Edwards et al., 2001; Dold, 2014).

The Jiko data fit this model well. The more altered rocks show both higher CIA values and clearer XRD evidence of Fe oxyhydroxides, while petrographic sections show Fe-oxide coatings along grain boundaries and fractures. The moderate positive relationships of soil Pb with Fe_2O_3 ($r = 0.390$) and MnO ($r = 0.541$) (Table 4) are also consistent with secondary adsorption or co-precipitation onto Fe-Mn-rich phases in the weathering profile. Thus, Fe oxyhydroxides at Jiko appear to play a dual role: they partly immobilise liberated Pb in soils, while also contributing to secondary transport where oxide-coated particles and colloids are mobilised by runoff or fluctuating redox conditions. This helps explain why high Pb concentrations can coexist in both soils and waters at the site. The Pb is not simply released once and removed; rather, it is repeatedly partitioned among primary minerals, pore waters, oxide coatings, suspended particulates, and surface waters along an evolving source-to-sink continuum.

4.5 Petrographic Evidence of Pb Mobilisation Pathways

The petrographic data provide direct micro-scale evidence of the pathways through which Pb is likely being released and redistributed. In the schistose rocks, the strong preferred orientation of mica laths creates a fabric that enhances permeability parallel to foliation and increases the exposed reactive surface area of cleavage planes. The frayed mica margins observed in thin section are consistent with early-stage alteration along structurally planes of weakness, which are precisely the domains most vulnerable to fluid-assisted leaching.

Likewise, the incipient sericitisation and turbidity of feldspar indicate hydrolytic destabilisation of the feldspar framework. In the more altered gneissic domain, the stronger fracturing of mica grains, pervasive feldspar alteration, and Fe-oxide-coated grain boundaries all point to a more advanced stage of mineral breakdown and secondary phase development. These textural characteristics show that Pb mobilisation at Jiko is controlled not only by mineral composition but also by microstructural fabric. This point is important in a mining environment. Artisanal excavation, blasting, crushing, and sediment reworking do not create the Pb source itself, but they substantially increase mineral surface area, fracture density, and exposure of reactive mineral domains to oxygenated meteoric waters. In this sense, mining acts as a kinetic accelerant of lithogenic Pb release. The petrographic textures therefore support a model in which natural basement weathering supplies the Pb, while artisanal disturbance enhances the rate and spatial extent of mobilisation in geochemical environments.

4.6 Integrated Source-to-Sink Model for Pb at Jiko

When the XRF, CIA, XRD, and petrographic datasets are considered together (Table 7), they define a coherent source-to-sink model (Table 8) for Pb mobilisation at Jiko. In the least altered rocks, Pb is retained mainly within the primary mineral framework, especially mica- and feldspar-bearing basement lithologies. As chemical weathering progresses, alkali depletion, mica-edge alteration, and feldspar hydrolysis release Pb into pore fluids. At the same time, oxidation of Fe-bearing minerals generates goethite and hematite, which capture part of the liberated Pb through adsorption and surface complexation. Continued weathering, physical disturbance, and hydrological flushing then redistribute Pb into the surrounding soil and surface-water system. This model is consistent with the strong correlation between MgO and soil Pb, the moderate CIA values, the transition from fresh to altered mineral assemblages in the XRD data, and the petrographic progression from fresh mica-feldspar textures to oxide-coated altered fabrics. It also explains why elevated Pb occurs in both soils and surface waters without requiring wholesale destruction of the bedrock mineralogy. Jiko therefore represents a case in which lithology controls the availability of Pb, while weathering and artisanal mining control its subsequent mobilisation and transfer among environmental media.

4.7 Geogenic versus Anthropogenic Control on Pb Enrichment

A major objective of this study was to distinguish whether Pb enrichment around the Jiko mine site is primarily geogenic or anthropogenic. The evidence strongly supports a model in which the dominant source is geogenic, but the mobilisation is enhanced by anthropogenic disturbance. The strongest support for a lithogenic origin is the very strong positive relationship between MgO and soil Pb, together with the mineralogical evidence for mica-rich basement lithologies and the weathering textures that show active release from primary minerals. If Pb were controlled mainly by random external contamination from surface processing (mining effect) alone, such systematic coupling with rock-forming major oxides would be less likely. Similarly, the moderate CIA values indicate that natural weathering of the basement is sufficient to release Pb without requiring extreme chemical alteration or acid mine drainage.

At the same time, the role of artisanal mining cannot be discounted. Excavation and reworking of mineralised rock and

alluvium greatly increase exposure of fresh surfaces and create efficient pathways for erosion, runoff, and particulate transport. Thus, our interpretation is that Jiko is a geogenically enriched system that has been anthropogenically accelerated. In source-apportionment terms, the mine workings are best regarded not as the sole origin of Pb, but as an important mechanism amplifying the mobility, redistribution, and environmental exposure of a naturally elevated Pb-bearing basement. A fully definitive distinction between different Pb sources would require additional advanced analytical techniques such as Pb isotope analysis, sequential extraction, and possibly reflected-light ore petrography. Nonetheless, the present multi-proxy evidence already provides a strong basis for concluding that the basement mineralogy is the primary control on Pb enrichment at the site.

4.8 Broader Geological and Environmental Geochemical Significance

The Jiko results fit a broader pattern observed in basement and mining terrains, where trace metals are not simply introduced from outside the system but are inherited from lithology and redistributed by weathering and human disturbance. Similar emphasis on distinguishing geogenic background from anthropogenic overprint has been made in source-apportionment studies of contaminated soils, including work showing that robust interpretation requires combined use of chemistry, mineralogy, and petrographic evidence rather than reliance on a single index alone (Algeo et al., 2025). For abandoned and semi-active mine sites in crystalline basement settings, this distinction matters greatly. If contamination is treated only as a mine-waste problem, remediation may overlook the wider lithological control on metal supply. At Jiko, the results suggest that Pb risk is likely to extend beyond the immediate mine pit area into the broader weathering and drainage system, especially where mica-rich and Fe-bearing basement rocks crop out and are seasonally flushed by runoff. This has clear implications for site assessment, mine closure, and environmental risk management in Jiko community, North-Central Nigeria and comparable Pan-African basement terrains. As per public health implications, the absence of a safe exposure threshold for Pb (ATSDR, 2020; WHO, 2021) underscores the significance of the elevated concentrations observed in this study.

Table 7: Synthesis of multi-proxy evidence supporting lithological control on Pb mobilisation at Jiko.

Evidence type	Key observation	Interpretation
Major oxide geochemistry	Moderate SiO_2, elevated Fe_2O_3 and TiO_2, low alkalis	Mafic- to intermediate-influenced basement with potential for naturally elevated Pb background
Correlation analysis	Strong MgO-soil Pb correlation; positive CaO-soil Pb relationship	Pb linked to Mg-Ca-bearing rock-forming minerals rather than random external contamination
CIA	Mean CIA indicates fresh to moderately weathered rock	Early chemical weathering is sufficient to initiate Pb release
XRD mineralogy	Quartz, phlogopite, albite, with goethite/hematite in altered samples	Primary silicate hosts release Pb; secondary Fe oxyhydroxides capture and redistribute it
Petrography	Frayed mica margins, feldspar turbidity, Fe-oxide grain-boundary coatings	Micro-scale evidence of Pb release, alteration, and secondary sequestration
Site condition	Artisanal excavation and sediment reworking	Mining acts mainly as an accelerant of lithogenic Pb mobilisation

Table 8: Conceptual stages of Pb mobilisation in the Jiko basement-weathering system.

Stage	Dominant Process	Principal Pb Form	Main Evidence
I. Primary storage	Pb retained in mica- and feldspar-bearing basement rocks	Lattice-bound/structurally associated Pb	Fresh mineral assemblages, low CIA, intact petrographic textures
II. Weathering release	Hydrolysis of feldspar and alteration of mica cleavage domains	Dissolved and pore-water Pb	Increasing CIA, feldspar turbidity, frayed mica margins
III. Secondary partitioning	Adsorption/co-precipitation on Fe oxyhydroxides and particulate transport	Oxide-bound and suspended Pb, plus residual dissolved Pb	Goethite-hematite by XRD, Fe-oxide coatings in thin section, elevated soil and water Pb

5. CONCLUSIONS

Understanding the controls on heavy metal mobilisation in abandoned mine environments is critical for effective environmental risk assessment, particularly within crystalline basement terrains where lithogenic contributions may be significant. This study investigates the lithological and mineralogical controls on lead (Pb) mobilisation at the abandoned Jiko mine site, North-Central Nigeria, using an integrated approach comprising X-ray Fluorescence (XRF), X-ray Diffraction (XRD), Chemical Index of Alteration (CIA), correlation analysis, and petrographic examination. The basement rocks exhibit an intermediate to mafic geochemical affinity, with elevated Fe_2O_3 (mean = 9.58 wt.%), TiO_2 (2.17 wt.%), and CaO (6.03 wt.%), consistent with schist belt lithologies known to host naturally elevated trace metals. Mineralogical analysis identifies quartz, phlogopite, and albite as dominant primary phases, with secondary goethite and hematite formed during weathering. A strong positive correlation between MgO and soil Pb (r = 0.817) provides robust evidence for a predominantly geogenic Pb source, hosted within mica and feldspar lattice structures. CIA values (48.35-62.20; mean = 54.15) indicate incipient to moderate weathering, sufficient to mobilise Pb from primary mineral lattices, while petrographic observations of frayed biotite, feldspar sericitisation, and Fe-oxide coatings reveal micro-scale pathways of Pb release and redistribution. The results define a three-stage mobilisation pathway: (i) primary lithogenic storage of Pb in silicate minerals; (ii) weathering-induced liberation of Pb^{2+} during hydrolytic alteration; and (iii) partial retention via adsorption onto secondary Fe oxyhydroxides, coupled with residual transport into surface waters. Structural controls associated with schistose fabric further enhance Pb leaching efficiency. Thus, the results indicate a coupled weathering–adsorption system in which Pb is first liberated from silicate lattices and subsequently partitioned between Fe-oxide-bound and dissolved phases.

These findings demonstrate that Pb enrichment is predominantly controlled by basement mineralogy, with artisanal mining acting as a secondary accelerant, thereby highlighting the need to explicitly consider geogenic baselines in contamination assessment. The elevated Pb mobility inferred from this study implies significant environmental and public health risks, particularly through soil-water exposure pathways in mining-impacted communities. Accordingly, this study recommends integrated monitoring and targeted remediation strategies, alongside advanced analytical approaches such as Pb isotopic fingerprinting and SEM-EDS microanalysis to refine source apportionment and support evidence-based environmental management in ASM-affected basement terrains.

6. ACKNOWLEDGEMENTS

The authors acknowledge the National Geosciences Research Laboratories (NGRL) of the Nigerian Geological Survey Agency (NGSA), Kaduna, Nigeria for conducting the XRF, XRD, and thin-section petrographic analyses. This work forms part of the undergraduate research of the lead author at the Federal University of Technology, Minna, Nigeria, where additional petrographic studies were undertaken. Appreciation is also extended to staff members who assisted with photomicrograph interpretations. This research received no specific grant from funding agencies in the public, commercial, or not-for-profit sectors.

7. REFERENCES

Adriano, D. C. (2001). *Trace Elements in Terrestrial Environments: Biogeochemistry, Bioavailability, and Risks of Metals* (2nd ed.). Springer, New York. **DOI:** https://doi.org/10.1007/978-0-387-21510-5

Agency for Toxic Substances and Disease Registry (ATSDR). (2020). *Toxicological Profile for Lead*. U.S. Department of Health and Human Services, Atlanta. Retrieved from https://www.atsdr.cdc.gov/toxprofiles/tp13.pdf

Ahmed, A. L., Hfiz, B., Umar, M., & Balarabe, B. (2020). Electrical Resistivity Investigation of Subsurface Structures at the N.Y.S.C. Proposed Permanent Orientation Camp, Paiko, Niger State. *FUDMA Journal of Sciences (FJS), 4(1), 301 – 320*. https://www.researchgate.net/publication/355369696

Algeo, T. J., Hong, H., & Wang, C. (2025). The chemical index of alteration (CIA) and interpretation of ACNK diagrams. *Chemical Geology*, 671, 122474. **DOI**: https://doi.org/10.1016/j.chemgeo.2024.122474

Alloway, B. J. (Ed.). (2013). *Heavy Metals in Soils: Trace Metals and Metalloids in Soils and their Bioavailability* (3rd ed.). Springer, Dordrecht. **DOI:** https://doi.org/10.1007/978-94-007-4470-7

Cornell, R. M., & Schwertmann, U. (2003). *The Iron Oxides: Structure, Properties, Reactions, Occurrences and Uses* (2nd ed.). Wiley-VCH, Weinheim. **DOI:** https://doi.org/10.1002/3527602097

Dold, B. (2014). Evolution of acid mine drainage formation in sulphidic mine tailings. *Minerals*, 4(3), 621–641. **DOI:** https://doi.org/10.3390/min4030621

Dooyema, C. A., Neri, A., Lo, Y. C., Durant, J., Dargan, P.I., Swarthout, T., … Brown, M, J. (2012). Outbreak of fatal childhood lead poisoning related to artisanal gold mining in northwestern Nigeria, 2010. *Environ Health Perspect*., 120(4), 601-7. **DOI**: https://pmc.ncbi.nlm.nih.gov/articles/PMC3339453/

Ettler, V. (2016). Soil contamination near non-ferrous metal smelters: A review. *Applied Geochemistry*, 64, 56–74. **DOI:** https://doi.org/10.1016/j.apgeochem.2015.09.020

Facchinelli, A., Sacchi, E., & Mallen, L. (2001). Multivariate statistical and GIS-based approach to identify heavy metal sources in soils. *Environmental Pollution*, 114(3), 313–324. **DOI:** https://doi.org/10.1016/S0269-7491(00)00243-8

Fashola, M. O., Ngole-Jeme, V. M., & Babalola, O. O. (2016). Heavy metal pollution from gold mines: Environmental effects and bacterial strategies for resistance. *International Journal of Environmental Research and Public Health*, 13(11), 1047. **DOI:** https://doi.org/10.3390/ijerph13111047

Förstner, U., & Wittmann, G. T. W. (1983). *Metal Pollution in the Aquatic Environment* (2nd ed.). Springer, Berlin. **DOI:** https://doi.org/10.1007/978-3-642-69385-4

Garba, I. (2003). Geochemical characteristics of mesothermal gold mineralisation in the Pan-African (600 ± 150 Ma) basement of Nigeria. *Applied Earth Science (Transactions of the Institution of Mining and Metallurgy, Section B)*, 112(3), 319–325. **DOI**: https://doi.org/10.1179/037174503225003143

Gottesfeld, P., Meltzer, G., Costello, S., Greig, J., Thurtle, N., Bil, K., Mwangombe, B. J., Nota, M. M. (2019). Declining blood lead levels among small-scale miners participating in a safer mining pilot programme in Nigeria. *Occup Environ Med*, 76(11), 849-853. **DOI**: https://oem.bmj.com/content/76/11/849

Håkanson, L. (1980). An ecological risk index for aquatic pollution control: A sedimentological approach. *Water Research*, 14(8), 975–1001. **DOI:** https://doi.org/10.1016/0043-1354(80)90143-8

Hawkes, H. E., & Webb, J. S. (1962). *Geochemistry in Mineral Exploration*. Harper & Row, New York.

Hilson, G. (2002). The environmental impact of small-scale gold mining in Ghana: Identifying problems and possible solutions. *The Geographical Journal*, 168(1), 57–72. **DOI:** https://doi.org/10.1111/1475-4959.00040

Hudson-Edwards, K. A., Macklin, M. G., & Taylor, M. P. (2001). 2000 years of sediment-borne heavy metal storage in the Yorkshire Ouse basin, NE England, UK. *Hydrological Processes*, 15(12), 1473–1491. **DOI:** https://doi.org/10.1002/hyp.207

Järup, L. (2003). Hazards of heavy metal contamination. *British Medical Bulletin*, 68(1), 167–182. **DOI:** https://doi.org/10.1093/bmb/ldg032

Johnson, D. B., & Hallberg, K. B. (2005). Acid mine drainage remediation options: A review. *Science of the Total Environment*, 338(1–2), 3–14. **DOI:** https://doi.org/10.1016/j.scitotenv.2004.09.002

Komárek, M., Ettler, V., Chrastný, V., & Mihaljevič, M. (2008). Lead isotopes in environmental sciences: A review. *Environment International*, 34(4), 562–577. **DOI:** https://doi.org/10.1016/j.envint.2007.10.005

Laidlaw, M. A. S., & Filippelli, G. M. (2008). Resuspension of urban soils as a persistent source of lead poisoning in children: A review and new directions. *Applied Geochemistry*, 23(8), 2021–2039. **DOI:** https://doi.org/10.1016/j.apgeochem.2008.04.020

Lanphear, B. P., Hornung, R., Khoury, J., Yolton, K., Baghurst, P., Bellinger, D. C., … Roberts, R. (2005). Low-level environmental lead exposure and children's intellectual function: An international pooled analysis. *Environmental Health Perspectives*, 113(7), 894–899. **DOI:** https://doi.org/10.1289/ehp.7688

Liu, C. W., Lin, K. H., & Kuo, Y. M. (2003). Application of factor analysis in the assessment of groundwater quality in a blackfoot disease area in Taiwan. *Science of the Total Environment*, 313(1–3), 77–89. **DOI:** https://doi.org/10.1016/S0048-9697(02)00683-6

McLennan, S. M. (1993). Weathering and global denudation. *The Journal of Geology*, 101(2), 295–303. DOI: https://doi.org/10.1086/648222

Müller, G. (1969). Index of geoaccumulation in sediments of the Rhine River. *GeoJournal*, 2(3), 108–118.

Nesbitt, H. W., & Young, G. M. (1982). Early Proterozoic climates and plate motions inferred from major element chemistry of lutites. *Nature*, 299(5885), 715–717. **DOI:** https://doi.org/10.1038/299715a0

Nesse, W. D. (2013). *Introduction to Optical Mineralogy* (4th ed.). Oxford University Press, New York. ISBN: 978-0199846276.

Nota, M. M., Gottesfeld, P., Mbuligwe, S. E., Kassenga, G. R., & Mohammed Anka, S. (2025). Airborne lead exposures during artisanal lead mining and gold ore processing in Zamfara, Nigeria. *Journal of Occupational and Environmental Hygiene*, 22(9), 726–732. **DOI**: https://doi.org/10.1080/15459624.2025.2491490

Obaje, N. G. (2009). *Geology and Mineral Resources of Nigeria*. Springer, Berlin. **DOI:** https://doi.org/10.1007/978-3-540-92685-6

Plumlee, G. S., Durant, J. T., Morman, S. A., Neri, A., Wolf, R. E., Dooyema, C. A., … Brown, M. J. (2013). Linking geological and health sciences to assess childhood lead poisoning from artisanal gold mining in Nigeria. *Environmental Health Perspectives*, 121(6), 744–750. **DOI:** https://doi.org/10.1289/ehp.1206051

Rahaman, M. A. (1988). Recent advances in the study of the Basement Complex of Nigeria. In P. O. Oluyide, W. C. Mbonu, & A. E. Ogezi (Eds.), *Precambrian Geology of Nigeria* (pp. 11–41). Geological Survey of Nigeria, Kaduna.

Rasheed, H., Suleiman, A., & Akande, W. G. (2026). Heavy metal contamination assessment in soils and surface waters around an abandoned mine site in Jiko Village, North-Central Nigeria. *Journal of Geoscience and Environment Protection*, 14(4), in press (accepted).

Reimann, C., & Filzmoser, P. (2000). Normal and lognormal data distribution in geochemistry: Death of a myth. *Environmental Geology*, 39(9), 1001–1014. **DOI:** https://doi.org/10.1007/s002540000116

Reimann, C., & Garrett, R. G. (2005). Geochemical background — concept and reality. *Science of the Total Environment*, 350(1–3), 12–27. **DOI:** https://doi.org/10.1016/j.scitotenv.2005.01.047

Salminen, R., & Tarvainen, T. (1997). The problem of defining geochemical baselines: A case study of selected elements and geological materials in Finland. *Journal of Geochemical Exploration*, 60(1), 91–98. **DOI:** https://doi.org/10.1016/S0375-6742(97)00028-2

Sutherland, R. A. (2000). Bed sediment-associated trace metals in an urban stream, Oahu, Hawaii. *Environmental Geology*, 39(6), 611–627. **DOI:** https://doi.org/10.1007/s002540050475

Taylor, S. R., & McLennan, S. M. (1985). *The Continental Crust: Its Composition and Evolution*. Blackwell Scientific Publications, Oxford. https://commons.library.stonybrook.edu/cgi/viewcontent.cgi?article=1011&context=geo-articles

Tchounwou, P. B., Yedjou, C. G., Patlolla, A. K., & Sutton, D. J. (2012). Heavy metal toxicity and the environment. *Experientia Supplementum*, 101, 133–164. **DOI:** https://doi.org/10.1007/978-3-7643-8340-4_6

Tessier, A., Campbell, P. G. C., & Bisson, M. (1979). Sequential extraction procedure for the speciation of particulate trace metals. *Analytical Chemistry*, 51(7), 844–851. **DOI:** https://doi.org/10.1021/ac50043a017

World Health Organization (WHO). (2021). *Lead poisoning and health*. WHO Fact Sheet. Retrieved from https://www.who.int/news-room/fact-sheets/detail/lead-poisoning-and-health

How to cite this article: Hammed Rasheed, Abdullahi Suleiman, and Waheed Gbenga Akande. Mineralogical Controls on Lead Mobilisation in a Basement Terrain: Integrated Geochemical and Petrographic Evidence from an Abandoned Mine Site, North-Central Nigeria. *Am. J. innov. res. appl. sci.* 2026, 22(4): 1-14. DOI: 10.5281/zenodo.19462180